Supplement of Atmos. Chem. Phys., 16, 2139–2153, 2016
http://www.atmos-chem-phys.net/16/2139/2016/
doi:10.5194/acp-16-2139-2016-supplement

Atmospheric Chemistry and Physics Open Access EGU

Supplement of

Secondary formation of nitrated phenols: insights from observations during the Uintah Basin Winter Ozone Study (UBWOS) 2014

B. Yuan et al.

Correspondence to: Bin Yuan (bin.yuan@noaa.gov)

1. Sensitivities of phenols in PTR-TOF

The sensitivities of VOC species *X* (S_X) in PTR-TOF are calculated as:

$$S_X = S_Y \times \frac{k_X}{k_Y} \qquad (1)$$

Here, S_Y is sensitivity of the surrogate species *Y*, which has a comparable mass in PTR-ToF as the species *X*. k_X and k_Y are the rate coefficients of the proton transfer reaction between the hydronium ion (H_3O^+) and X (or Y), respectively.

Table S1. Determination of sensitivities of phenols from the calibrated aromatic compounds

Target species			Surrogate species		
Name	k^b, 10^{-9} cm^3 molecule^{-1} s^{-1}	Sensitivity, ncps/ppb	Name	k, 10^{-9} cm^3 molecule^{-1} s^{-1}	Sensitivity, ncps/ppb
Phenol	2.18	23.0	Toluene	2.08	21.9
Cresol	2.30	25.7	C8-aromatics	2.26	25.2
DMP[a]	N/A	21.7	C9-aromatics	2.40	21.7

a: DMP indicates dimethylphenols.

b: Proton transfer reaction rate coefficients between the hydronium ion (H_3O^+) and selected VOCs (Cappellin et al., 2012).

2. Gas-particle partitioning

The fraction in particles (F_p) for a species X can be expressed as:

$$F_p = \frac{c_p}{c_g + c_p}$$

where c_g and c_p are concentrations of the species in the gas phase and particle phase, respectively. F_p can be calculated based on the equilibrium absorption partitioning theory:

$$F_p = (1 + \frac{C^*}{C_{OA}})^{-1}$$

where C_{OA} is the concentrations of organic aerosol (OA). C^* is the effective saturation mass concentration, which is calculated as:

$$C^* = \frac{M 10^6 \zeta P_V}{760 RT}$$

where M (g mol^{-1}) is the molecular weight of the species, P_V is pure-compound liquid vapor pressure in Torr. ζ is the activity coefficient of the species in the OA mixture (assumed =1). R is the gas constant (8.2×10^{-5} m^3 atm K^{-1} mol^{-1}). T is ambient temperature in K.

The dependence of vapor pressure is accounted for using the Clausius-Clapeyron relationship with reported enthalpies of evaporation (ΔH_{vap}) (Schwarzenbach et al., 1988).

$$P_V = P_{V,0}\exp\left[\frac{\Delta H_{vap}}{R}\left(\frac{1}{T_0}-\frac{1}{T}\right)\right]$$

where P_V (Torr) and $P_{V,0}$ (Torr) is vapor pressure of the species at temperature T (K) and at reference temperature T_0 (K), respectively.

The uptake rate (R_{in}) and volatilization rate (R_{out}) of a gas phase species by particles with radius r are approximated by (Jacob, 2000):

$$R_{in} = \left(\frac{r}{D_g}+\frac{4}{\upsilon\alpha}\right)^{-1} A\times c_g$$

$$R_{out} = \left(\frac{r}{D_g}+\frac{4}{\upsilon\alpha}\right)^{-1} A\times \frac{c_p}{K_{ep}}$$

where D_g is the gas-phase molecular diffusion coefficient (m^2 s^{-1}), υ is the mean molecular speed (m s^{-1}), α is the mass accommodation coefficient, A is the aerosol surface area per unit volume of air (m^2 m^{-3}). K_{ep} is the equilibrium constant, i.e. c_p/c_g, or $F_p/(1-F_p)$. The characteristic time scales of mass transfer are of the order minutes for particles in the troposphere (Bowman et al., 1997;Jacob, 2000). Here, we assume that the equilibrium is maintained at each model step (5 min).

Table S2. Concentrationsof VOCs, NO_x and ozone in Jan. 18-27 during the UBWOS 2014 campaign (average±standard deviation).

Species	Conc., ppb	Species	Conc., ppb
Methane	$6.23\pm2.56\times10^3$	Ethyne	1.89±0.89
Ethane	214.8±110.5	Benzene	3.03±1.48
Propane	128.5±67.7	Toluene	3.90±1.92
n-Butane	52.5±28. 9	o-xylene	0.33±0.17
Isobutane	30.6±16.7	m+p-xylenes	1.33±0.71
n-Pentane	23.2±13.8	Ethylbenzene	0.26±0.13
isopentane	22.8±13.4	1,2,4-TMB	0.13±0.09
n-Hexane	11.3±6.41	1,2,3-TMB	0.04±0.04
2-Methylpentane	3.18±1.88	1,3,5-TMB	0.07±0.06
3-Methylpentane	9.58±5.80	n-propylbenzene	0.02±0.02
2,2-dimethylButane	0.56±0.28	i-propylbenzene	0.02±0.01
n-Heptane	5.78±3.30	2-methyl-1ethylbenzene	0.01±0.01
3-methylhexane	2.22±1.42	3+4-methyl-1ethylbenzene	0.12±0.06
n-Octane	2.29±1.26	Methanol	19.2±10.0
n-Nonane	0.46±0.42	Ethanol	2.56±7.39
n-Decane	0.34±0.16	Acetone	4.07±1.59
Cyclopentane	1.80±1.40	MEK	1.86±0.87
Cyclohexane	5.35±3.00	Acetadehyde	2.54±1.23
Methylcyclopentane	5.47±3.69	Propanal	0.68±0.26
Ethlycyclohexane	0.69±0.52	n-Butanal	0.11±0.04
Ethene	1.69±0.80	NO	0.84±2.15
Propene	0.12±0.06	NO_2	5.15±3.07
1-Butene	0.01±0.01	O_3	51.7±13.2

TMB: trimethylbenzene.

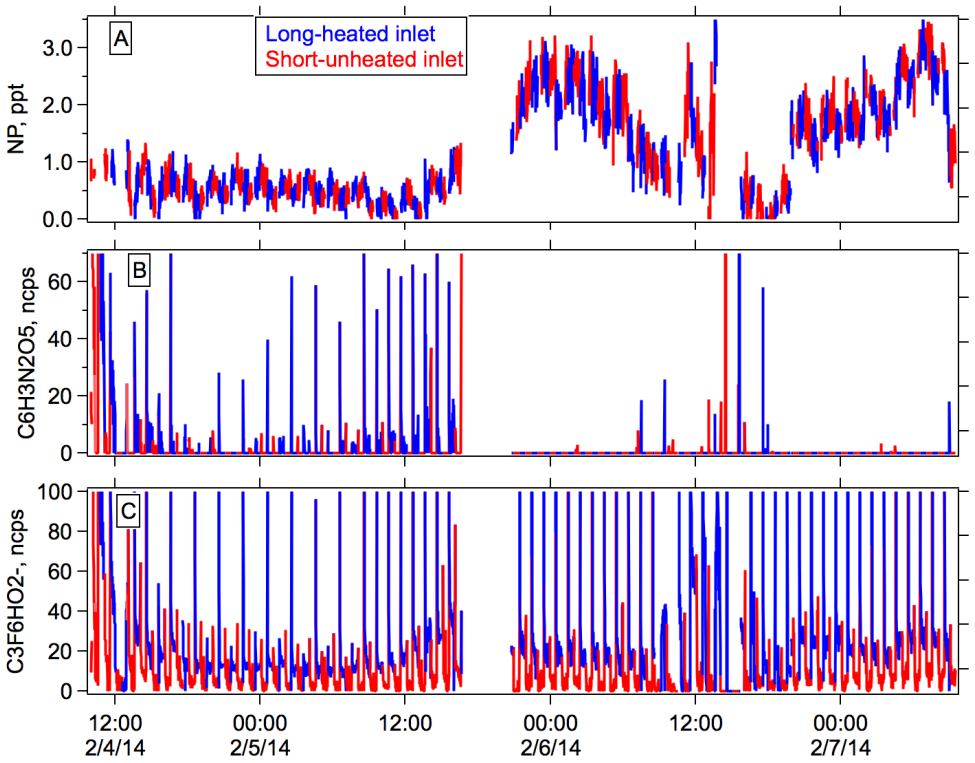

Fig. S1. Comparison of concentrations of NP (A) and the signals of $C_6H_3N_2O_5^-$ (*m/z* 183.0047, the masses for DNP) (B) and $C_3F_6HO_2^-$ (*m/z* 182.9886) (C) measured from a long-heated inlet and a short-unheated inlet. The spikes when switching to the other inlet in B and C were also observed for some fluorine ions in the acetate CIMS (e.g. *m/z* 112.9856 $C_2F_3O_2^-$, *m/z* 143.9840 $C_3F_4O_2^-$ and *m/z* 162.9824 $C_3F_5O_2^-$), which were believed to be Teflon impurity (Veres et al., 2010).

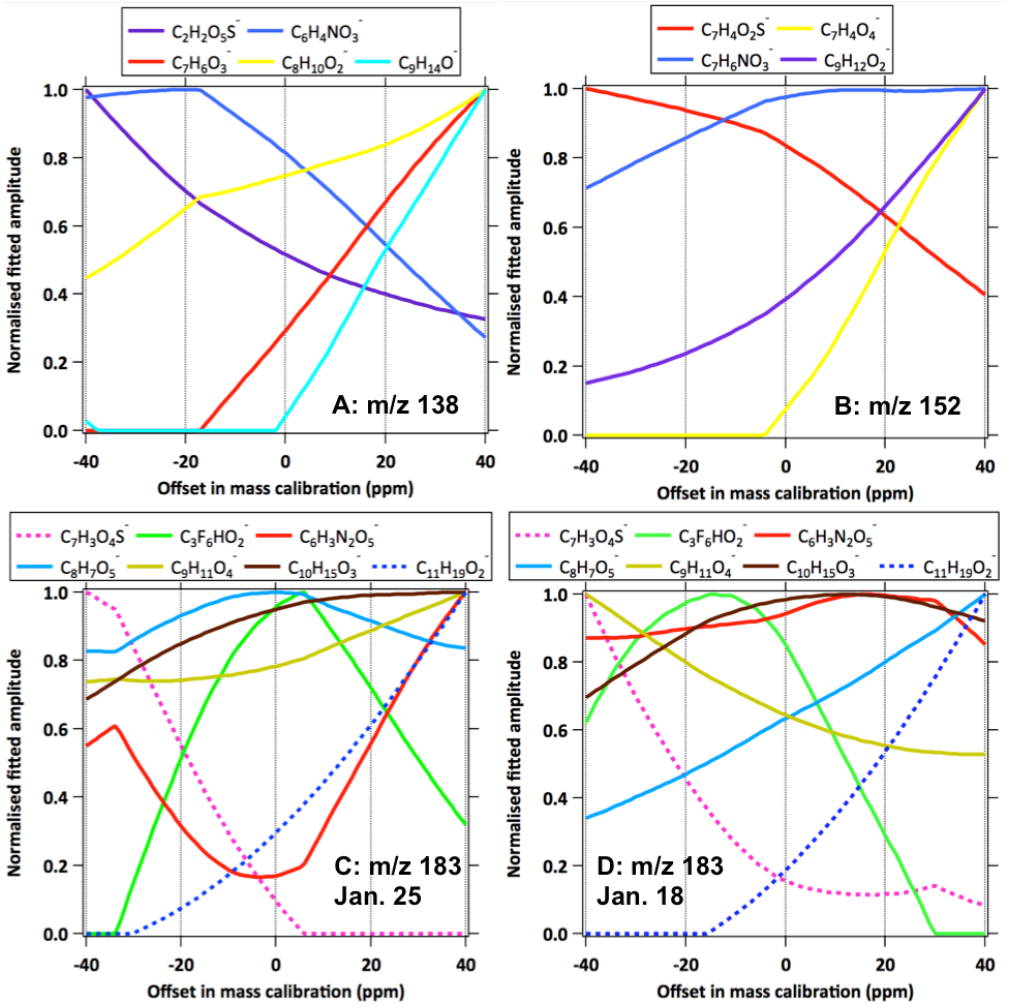

Figure S2. Sensitivity of the fitted ion intensities to mass calibration errors for ions at *m/z* 138 (A), *m/z* 152 (B) and *m/z* 183 (C) based on the averaged mass spectra on January 25, 2014 and *m/z* 183 (D) based on the averaged mass spectra on January 18, 2014 (see mass spectra in Figure 2). The results in the plots were obtained by (1) shifting the measured mass spectra by varying amount (from -40 ppm to 40 ppm) and (2) conducting peak fitting to the shifted mass spectra using the same ion locations calculated from their formula (Stark et al., 2015). The fitted signals relative to the maximum signals obtained between -40 ppm and 40 ppm are shown for each individual ion. The accuracy of mass calibration was 4.7±1.9 ppm for the whole campaign and the errors of mass calibration for individual ions were usually within 10 ppm (average+3σ).

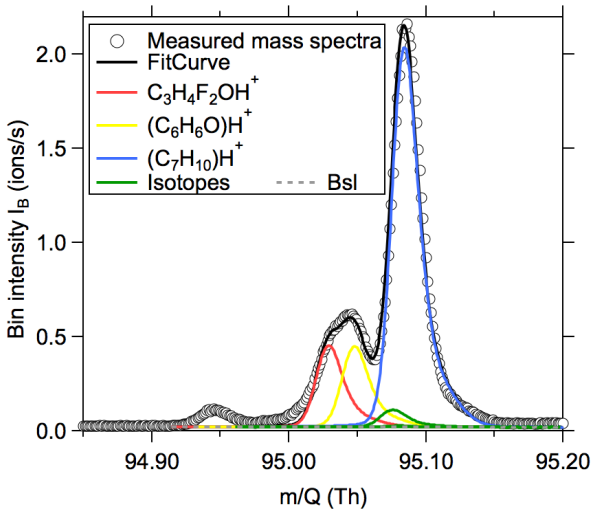

Figure S3. High-resolution peak fitting to the averaged mass spectra of *m/z* 95 collected by PTR-TOF on January 25, 2014 during the UBWOS 2014 campaign.

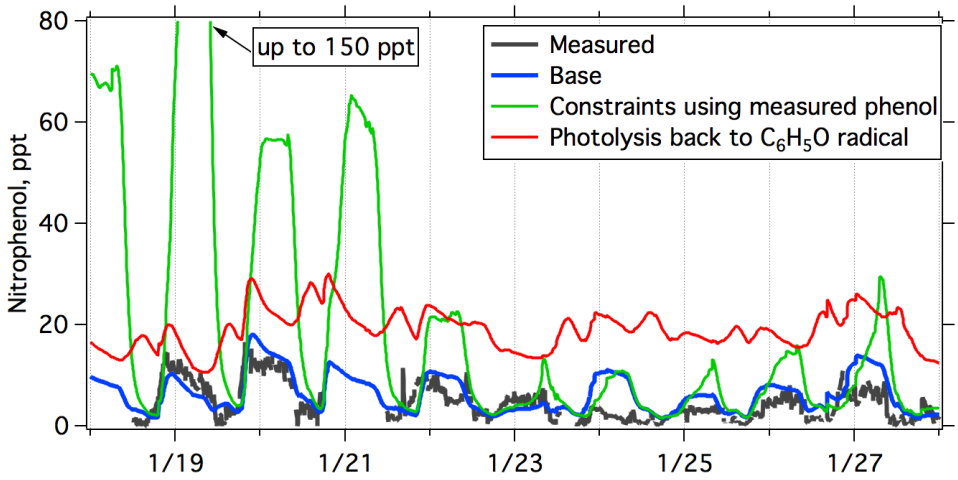

Figure S4. Comparison of measured and modeled time series of NP from the base simulation, a simulation using measured phenol concentrations as constraints, and a simulation assuming photolysis of NP only generates phenoxy (C_6H_5O) radicals.

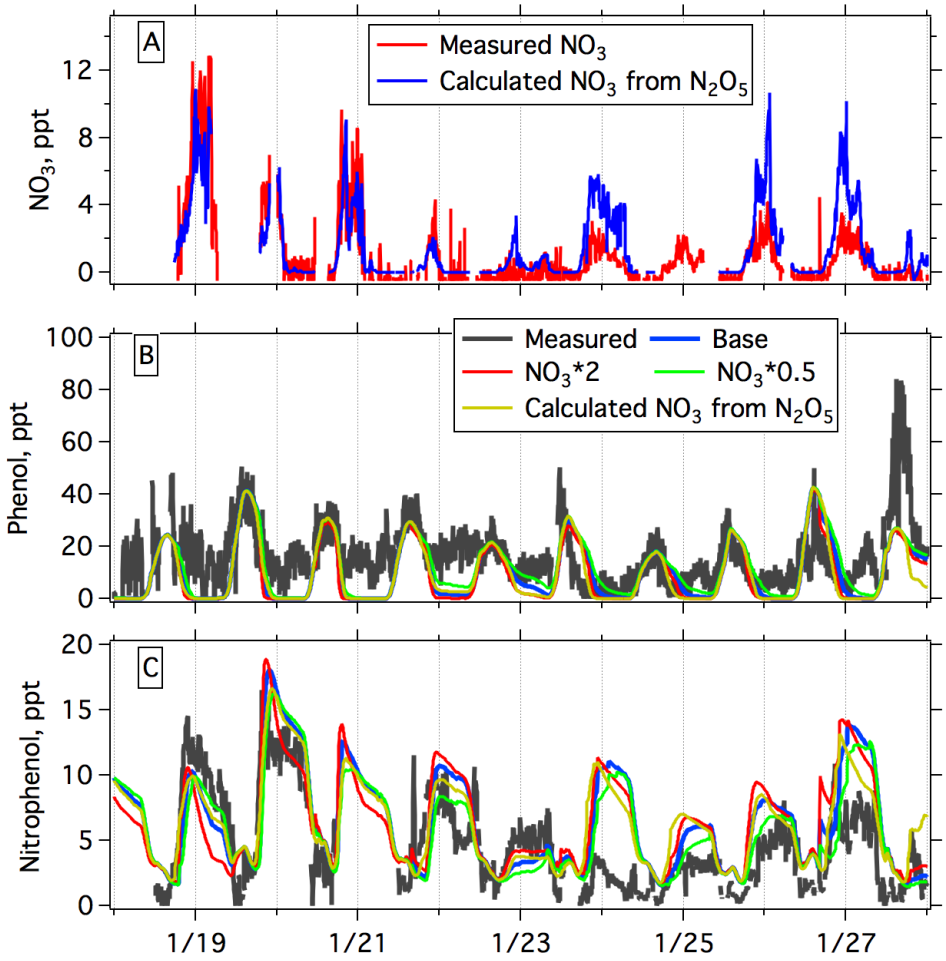

Figure S5. (A) Time series of measured NO_3 concentrations and NO_3 concentrations calculated based on the equilibrium between N_2O_5 and NO_3 (Brown et al., 2003). (B and C) Comparison of measured and modeled time series of phenol (B) and NP (C) from the base simulation, and simulations using constraints by varying measured NO_3 concentrations by a factor of 2 and using predicted NO_3 concentrations from N_2O_5 concentration as constraints.

Reference:

Bowman, F. M., Odum, J. R., Seinfeld, J. H., and Pandis, S. N.: Mathematical model for gas-particle partitioning of secondary organic aerosols, Atmospheric Environment, 31, 3921-3931, http://dx.doi.org/10.1016/S1352-2310(97)00245-8, 1997.

Brown, S. S., Stark, H., and Ravishankara, A. R.: Applicability of the steady state approximation to the interpretation of atmospheric observations of NO3 and N2O5, J. Geophys. Res., 108, doi: 10.1029/2003jd003407, 10.1029/2003jd003407, 2003.

Cappellin, L., Karl, T., Probst, M., Ismailova, O., Winkler, P. M., Soukoulis, C., Aprea, E., Mark, T. D., Gasperi, F., and Biasioli, F.: On quantitative determination of volatile organic compound concentrations using proton transfer reaction time-of-flight mass spectrometry, Environ Sci Technol, 46, 2283-2290, 10.1021/es203985t, 2012.

Jacob, D. J.: Heterogeneous chemistry and tropospheric ozone, Atmospheric Environment, 34, 2131-2159, http://dx.doi.org/10.1016/S1352-2310(99)00462-8, 2000.

Schwarzenbach, R. P., Stierli, R., Folsom, B. R., and Zeyer, J.: Compound properties relevant for assessing the environmental partitioning of nitrophenols, Environmental Science & Technology, 22, 83-92, 10.1021/es00166a009, 1988.

Stark, H., Yatavelli, R. L. N., Thompson, S. L., Kimmel, J. R., Cubison, M. J., Chhabra, P. S., Canagaratna, M. R., Jayne, J. T., Worsnop, D. R., and Jimenez, J. L.: Methods to extract molecular and bulk chemical information from series of complex mass spectra with limited mass resolution, International Journal of Mass Spectrometry, 10.1016/j.ijms.2015.08.011, 2015.

Veres, P., Roberts, J. M., Burling, I. R., Warneke, C., de Gouw, J., and Yokelson, R. J.: Measurements of gas-phase inorganic and organic acids from biomass fires by negative-ion proton-transfer chemical-ionization mass spectrometry, J. Geophys. Res., 115, doi:10.1029/2010JD014033, 10.1029/2010jd014033, 2010.